Hirshorn et al., Responses to Reviewer 1

The authors of this paper would like to thank the reviewer for their insightful and constructive comments on the paper. We have carefully considered the feedback and this resulted in major improvements to the paper. Please note that references to line numbers in the author responses correspond to the new line numbers in the updated manuscript.

The authors have color coded the responses to the reviewer as follows:

Blue: A response to the reviewer.
Black: Text that is in the originally submitted manuscript.
Red: Changes that were made to the manuscript and are reflected in the updated manuscript.

Major Comments

1. I suggest the authors to improve methodology section (specific comments below). Specially, it is not clear how the authors account the contribution of NPF to CCN, and only the timing of the events is presented.

Response: Lines 279 – 289 now include information on how we consider the contribution of NPF to CCN so that methods that detail the timing of CCN consideration, as well as how we compare CCN from events to non-events, are now included. We aim to highlight how this robust approach can be used in similar studies with long-term datasets.

Addition: To compare the impact NPF events have on CCN, CCN number concentrations directly measured are considered during the time period spanning from CCN_{start} to CCN_{end} during valid events and non-events. An average CCN number concentration for supersaturation levels between 0.2% and 0.4% is calculated for each individual time period. These values are then averaged each season separately between events and non-events. The goal is to determine whether CCN concentrations are enhanced by NPF events. During long-term studies, especially at clean, remote locations like SPL, directly comparing events and non-events will result in the relative enhancement of CCN due to events at a given location. By removing the subjectivity of selecting idealized cases, we provide a more robust methodology to evaluate long-term datasets. The methodology within this paper carefully considers similar timeframes within the diel pattern with and without NPF, to look at the relative change induced by NPF. By further comparing events to non-events through a seasonal lens, we ensure that days with similar meteorological conditions are compared. By further comparing events to non-events through a seasonal lens, we ensure that days with similar meteorological conditions are compared.

2. This manuscript presents a new methodology to classify NPF events, however it has been only applied at SPL site and validation, success ratio and/or comparison with other methods in detail are not provided. Despite it is a visual classification and can lead to human biases, Dal Maso et al 2005 has been used for years as an standardized method to classify NPF events. This methodology is presented as new, however it is based on Dal

Maso et al methodology. Why not comparing results in deep? This is not the first automatic method in the literature (e.g. Su et al., 2022) and no comparison, benefits or improvements are shown. Finally, the authors don't provide the procedure to calculate the GR, the formation rate is calculated with a formula that is simplified (and not correct), the diffusion coefficient is assumed to be 0.077 cm2 s-1 (this factor depends on the temperature and pressure, how representative is for SPL?) and the factor beta is also considered to be unity (why?). Kulmala et al 2012 provided guidelines to compare different NPF studies.

Response: One aspect that was often revisited when conducting this work was the subjectivity of both visual and automatic classification. We completely agree that Dal Maso et al., 2005 is a quintessential paper in our field, but there is a reliance on expert visual classifiers that are often not available or subjective. The goal of our statistical based method here is to provide a way that long-term datasets can be classified in a more efficient manner. It would be impossible to not consider Dal Maso et al., 2005 when creating the method which is why we provide a general comparison of the results of the automatic method to visual classification in section 5 of the paper. The goal here is to highlight the comparability of two methods while also acknowledging that discrepancies will occur due to the slightly different approaches of both methods. While Dal Maso et al., 2005 has been used for a longer period of time, we do believe that the promise of a more statistical-based and efficient way to classify NPF is why it is important to develop a statistical based method.

While a comparison with the automatic methods that use convolution neural networks (Joutsensaari et al., 2018; Su et al., 2022) was considered, we did not want to train the neural network with data classified by the statistical method in our study. For example, Su et al., 2022 requires 358 annotated days to train and only classifies class 1 (banana shaped) events while our method can also identify class II days. Joutsensaari et al., 2018 presents another option of automatic classification using deep learning but recommends 150 days per class to properly train the method for each site. The big advantage of our method compared to other automatic methods is that aspects of the statistical method can be altered to fit individual sites without having to train the method.

The growth rate of an NPF event is found by finding the slope of the linear regression that is fit to the maximum Gaussians. This procedure follows the conventional growth rate equation by using the growth pattern observed in the Gaussian maximums. The equation and a more detailed explanation can now be found on lines 180-190 and in the figure below.

Addition: For days that are defined as an event, the growth rate and event start and stop times are calculated. The growth rate is determined by the following equation which uses the linear regression fit to the maximum Gaussians:

$$GR = \frac{d}{dt}\left(D_p\right) = \frac{\Delta D_p}{\Delta dt} \qquad (2)$$

Because the slope of the linear regression fit of the maximum Gaussians represents particle growth over time during NPF events, this value is used when determining the growth rate ~~finding the slope of the linear fit of the size-bin maxima~~. Derivatives of the linear regressions are used to determine the start and end time of events, where the start time of the event is defined by the time of the first maximum of the first-order derivative, and the end time of the event is defined by the time of the last first-order derivative minimum. Figure 3 illustrates an example of an NPF event, and a day classified as a non-event.

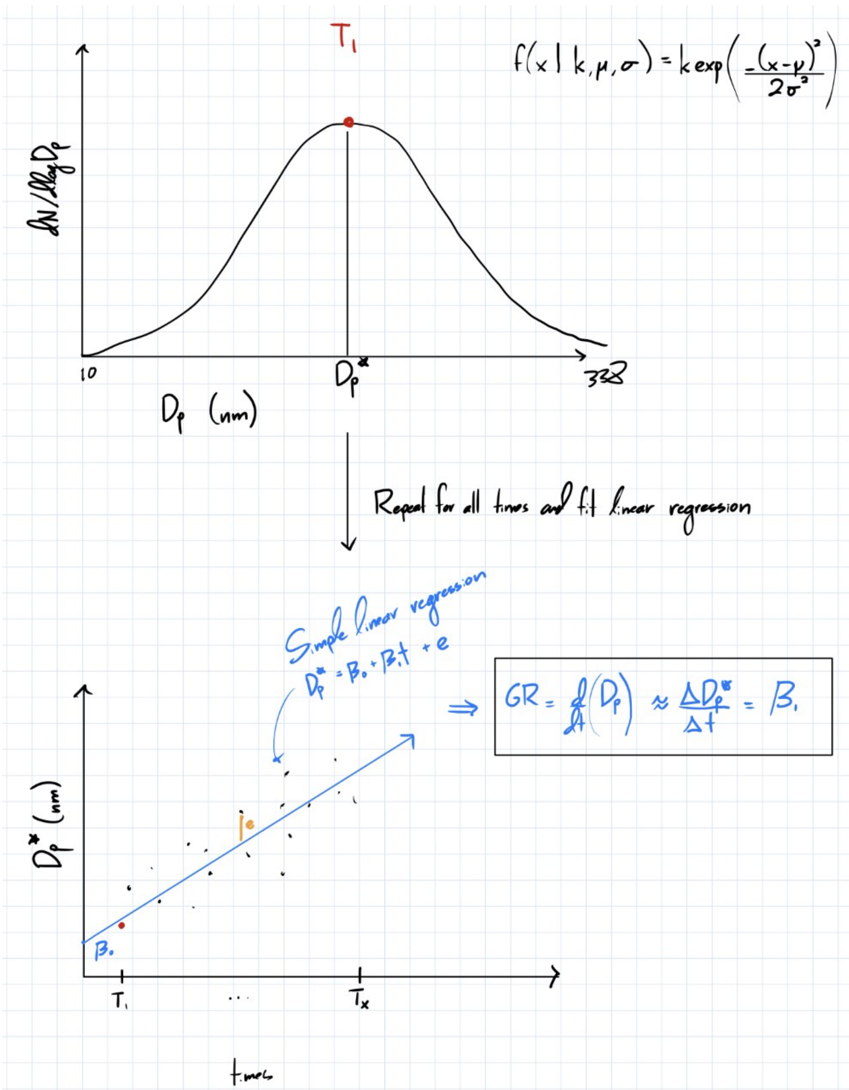

For the J_8 equation, the authors acknowledge that the equation we use is simplified. To maintain consistency across studies, we use the simplified form of the equation to mirror the work of Hallar et al., 2011 which uses Kulmala et al., 2004 to justify using the equation focused on sources while not considering sinks because of the clean conditions at SPL. A reference to Hallar et al., 2011 is added on line 227 to acknowledge that we also use this paper for justifying the equation. The values we get are different than Hallar et al., 2011, but we do believe that this has to do more with the time period considered in the calculations which is now determined through the automatic classification method. Lines 221 – 228 in the paper describe the protocol which we clearly outline to ensure the reader understands how we calculate the formation rate.

Addition: Where ~~N~~ $\Delta N_{8,Dmax}$ is the change in the number concentration of particles across the size distribution from about 8 nm to the maximum diameter (about 340 nm)~~, and~~ during Δt which is the time difference from the defined start of an event to the defined end of an event. When calculating the initial and final number concentrations, we utilize the average number concentration observed between 4 hours and 1 hour prior to NPF initiation as the initial number concentration. The final number concentration is the average number concentration from all 5-min scans taken during an event. Doing so allows for the comparison of the initial conditions of an NPF event, and aerosol formation across the entirety of a given event. We use the above formation rate equation because conditions at SPL are conducive to clean, homogenous air masses allowing for the use of the simplified version of the equation (Kulmala et al., 2004; Hallar et al., 2011).

Thank you for pointing out the error in the CS calculation. We have spent time revisiting the calculation for the diffusion coefficient and β. Below is a step by step process that details how we came up with a representative diffusion coefficient (0.13 $cm^2 s^{-1}$) as well as how we calculate β for each dataset:

The condensation sink in this work is calculated using the following equation (Kulmala et al., 2012):

$$CS = 2\pi D \int_0^\infty d_p \beta_m(d_p) n(d_p) dd_p = 4\pi D \sum_i \beta_i r_i N_i$$

In the equation, r is the radius of a given size bin (cm), N is the number concentration ($\#/cm^3$), D is the diffusion coefficient of H_2SO_4 (cm^2/s), and β is the transition regime correction. Both D and β are calculated out for SPL.

β can be calculated using the following equation (Kulmala et al., 2012; Tuovinen et al., 2020):

$$\beta = \frac{1 + kn}{1 + 0.377Kn + \frac{4}{3}\alpha^{-1}Kn + \frac{4}{3}\alpha^{-1}Kn^2}$$

Where α is the mass accommodation coefficient which is assumed to be unity in order to mirror previous work by Hallar et al., 2011. Kn is the Knudsen number which can be calculated by λ_v/r and will be a unique value at each radius. Radius must be in units of meters in this equation for the units to work. The following equation is used to calculate λ_v:

$$\lambda_v = 3\sqrt{\frac{\pi m_v}{8kT}} * D$$

D is the diffusion coefficient of vapor (m^2/s), k is the Boltzmann number (m^2kg/s^2K), T is the temperature in Kelvin (seasonal average temperature used for each given dataset), and m_v is the molecular mass of H_2SO_4 (Kg).

The value of D is assumed to be 0.13 cm^2s^{-1} after using representative data for SPL (680 mb pressure, -25 to 25 degrees C temperature range) and plugging these values into the following equation (Tuovinen et al., 2021, Welty et al., 2020):

$$D = \frac{10^{-3} T^{1.75} \sqrt{\frac{1}{M_{air}} + \frac{1}{M_{vapor}}}}{p\left(\sum_{v,air}^{1/3} + \sum_{v,vapor}^{1/3}\right)^2}$$

M_{air} and M_{vapor} are molecular weights in (g mol^{-1}) of each respective gas. T is the absolute temperature in Kelvin, $\Sigma_{v,air}$ and $\Sigma_{v,vapor}$ are diffusivity volumes of the air, and the condensing vapor molecule. P is pressure in standard atmosphere pressure (atm).

Lines 235-241 have been updated to address how we calculate both variables and the correct values of CS are updated in the paper.

Addition: ~~Where *D* is the diffusion coefficient of vapor, which we assume to be 0.077 cm^2s^{-1} for H_2SO_4 (Hanson and Eisele, 2000),~~ In the equation, r_i is the radius of a given size bin (cm), and N_i is the number concentration (#/cm^3) of the given size bin. *D* is the diffusion coefficient of vapor, which is assumed to be 0.13 cm^2s^{-1} for H_2SO_4 at SPL based on calculations using representative pressure and temperature at the site (Hanson and Eisele, 2000; Welty et al., 2020; Tuovinen et al., 2021). β_m is calculated following the protocols of Kulmala et al., 2012 and Tuovinen et al., 2020 (Kulmala et al., 2001; Nishita et al., 2008; Hallar et al., 2011; Kulmala et al., 2012; Tuovinen et al., 2020).

Because much of the work to calculate these variables was conducted by Gerardo Carrillo-Cardenas, he has been added as a co-author to the paper.

3. When talking about the impact of NPF to CCN concentrations, this method is not well explained and further explanations are needed. In addition, this method does not show clear advantages with those previously presented in the literature and I suggest the authors

to look in deep some of the issues discussed in previous works (e.g. Dameto de España et al., 2017; Rejano et al., 2021; Rose et al., 2017).

The authors would like to first acknowledge that the work conducted in the three previous papers helped to influence the method we have created to identify when to consider CCN as being enhanced by NPF. Below we have included a short summary of each of the aforementioned studies:

- Dameto de España et al., 2017: Two years of data with 38 events that have concurrent CCN measurements. 15 days were analyzed for CCN. The study uses a CCNC and tracks the time it takes from NPF initiation to CCN relevant sizes (time period 1) and considers CCN as enhanced by NPF for a time period the same length as time period 1. In addition, an event must have consistent traffic emissions concentrations, a consistent wind direction, and a stable mixing layer height.
- Rose et al., 2017: Data throughout 2012 with 94 analyzed NPF events. The study did not have a CCNC available. To consider CCN enhancements, the study utilizes a methodology to identify times in which NPF contributes to CCN concentrations, starting from when aerosol number concentrations at 50 nm, 80 nm, and 100 nm begin to increase and ending when the maximum number concentration is observed at the respective size bin.
- Rejano et al., 2021: Two years of data at two different sites. 15 of the clearest NPF days considered that display banana growth. The study did have a CCNC; however, the N_{CCN} was also estimated using aerosol properties (optical and from the size distribution).

When comparing our study to Dameto de España et al., 2017, Rejano et al., 2021, and Rose et al., 2017, a notable difference between the data available in each study is that our dataset spans 15 years compared to either 1 or 2 years in the aforementioned studies. Because of the length of our dataset, we aimed to define a series of thresholds that could easily be applied to size distributions to identify times starting when enough particles from an NPF event hit CCN relevant sizes (CCN_{start}) and ending when the growth of an event tapers off (CCN_{end}). The advantages of this method specifically compared to the above studies is that these thresholds can be applied to large datasets to identify the time which to consider CCN efficiently. Furthermore, only the size distribution is considered when identifying the CCN consideration times in our work which allow for a higher number of days to be considered.

Of the above methods, Dameto de España et al., 2017's paper appears to be the most similar because we both base the start time of CCN consideration on a time when particles reach CCN sizes. Because their work took place in Vienna, Austria there are multiple protocols to remove days influenced by urban emissions which could taint the NPF event. Due to SPL's remote location, we do not consider protocols in the same way as Dameto de España et al... Rather, we analyze the long-term growth of events and end CCN consideration when a given NPF event stops growing.

We acknowledge that there are differences between NPF events within our study, but we do believe that the high number of days considered by the study will ensure that any tainted days, which are less likely to occur in a remote location, will have a minimal effect on the data allowing for a comprehensive analysis of the enhancement of CCN due to NPF events.

Based on the above analysis and discussion, we believe our study has the following advantages making it important to get into the body of literature:

- Start and end times of CCN consideration are both considered based on the growth of particles in a given particle size distribution.
- By considering a higher number of days and splitting data into seasonal categories, we create a comprehensive and honest analysis of NPF's enhancement of CCN. We consider NPF events (type 1) some of which are clear type 1a events and others are weaker type 1b events. However, both occur at SPL and by considering both we can narrow in on the true enhancement of CCN.
- Determining CCN consideration times can be quickly done for large datasets eliminating the need for visual analysis of each day.

1) We can assume that all the particles >100nm will act as CCN, however not all particles below 100nm come from NPF events, so you can explore some subtracting method to account for that?

3) Free troposphere conditions will probably reduce the number of NPF events, and boundary layer conditions will lead to higher event frequency, why not using same atmospheric conditions to subtract the effect from lower sizes? 4) SMPS measures from 8 to 340 nm, if above 100nm we have the largest contribution to CCN concentrations, which errors have the increase factors that you present here?

These are both great points that the reviewer brings up. Given the clean conditions of SPL, the consideration of event vs. non-event days will help to address this concern. While particles above 100 nm will be present during both events and non-events, the comparison of the two will highlight the differences between the two classification categories while minimizing the effect of days that could negatively impact the comparison. Particles above 100 nm are considered within the aerosol size distribution for each individual day when determining when to consider CCN concentrations. We ensure that this detail is present on lines 250-251. The high number of days considered will result in a normalized comparison of events (type 1a and type 1b) vs. non-events. The methodology within this paper carefully considers similar timeframes within the diel pattern with and without NPF, to look at the relative change induced by NPF. Additional lines describing the importance of the comparison of events and non-event is added on 283 – 289.

Lines 253-254: For days classified as type 1a events and type 1b events, the start time of CCN consideration (CCN_{start}) is the first time after the start of an NPF event that 25% of all particles in a given scan (ranging from 8 nm to about 340 nm) are above 40 nm.

Addition: During long-term studies, especially at clean, remote locations like SPL, directly comparing events and non-events will result in the relative enhancement of CCN due to events at a given location. By removing the subjectivity of selecting idealized cases, we provide a more robust methodology to evaluate long-term datasets. The methodology within this paper carefully considers similar timeframes within the diel pattern with and without NPF, to look at the relative change induced by NPF. By further comparing events to non-events through a seasonal lens, we ensure that days with similar meteorological conditions are compared. By further comparing events to non-events through a seasonal lens, we ensure that days with similar meteorological conditions are compared.

2) SPL is a mountain site, the difference between event and non-event days will probably be affected by the transport from lower altitudes, I suggest to add some results/discussion about free troposphere conditions, influence from boundary layer, and the differences during event and non-event days.

Diel patterns of aerosols at Storm Peak Laboratory have previously been attributed to almost daily transitions of boundary layer and free tropospheric air masses at Storm Peak Laboratory (Borys and Wetzel, 1997). Since radiosondes are not commonly launched within the near vicinity of Storm Peak Laboratory, we have no representative potential temperature profiles and we therefore generally refer to nighttime air masses as regional air masses, although they may represent free tropospheric air as shown in previous studies (Borys and Wetzel, 1997, Borys et al., 1986). Generally data suggest a minimum concentrations of condensation nuclei (CN) in the early mornings which are considered background tropospheric concentrations (Lowenthal et al., 2002, Richardson et al., 2007; Obrist et al., 2008). Thus, the methodology within this paper carefully considers similar timeframes within the diel pattern with and without NPF, to look at the relative change induced by NPF.

References:

R.D. Borys, M.A. Wetzel; Storm Peak Laboratory: a research, teaching and service facility for the atmospheric sciences; Bulletin of the American Meteorological Society, 78 (1997), pp. 2115-2123.

R.D. Borys, D.H. Lowenthal, K.A. Rahn; Contributions of Smelters and Other Sources to pollution of sulfate at a mountaintop site in northwestern Colorado. Acid Deposition in Colorado – Local Versus Long-Distance Transport into the State; CIRA, Colorado State University, Ft. Collins, CO (1986); pp. 167–174.

D.H. Lowenthal, R.D. Borys, M.A. Wetzel; Aerosol distributions and cloud interactions at a mountaintop laboratory; Journal of Geophysical Research, 107 (2002), p. 4345, 10.1029/2001JD002046

M.S. Richardson, P.J. DeMott, S.M. Kreidenweis, D.J. Cziczo, E.J. Dunlea, J.L.Jimenez, D.S. Thomson, L.L. Ashbaugh, R.D. Borys, D.L. Westphal, G.S. Casuccio, T.L. Lersch; Measurements of heterogeneous ice nuclei in the western United States in springtime and their relation to aerosol characteristics; Journal of Geophysical Research – Atmospheres, 112 (D2) (2007), p. D02209

Obrist, D., Hallar, A. G., McCubbin, I., Stephens, B. B., & Rahn, T. (2008). Atmospheric mercury concentrations at Storm Peak Laboratory in the Rocky Mountains: Evidence for long-range transport from Asia, boundary layer contributions, and plant mercury uptake. *Atmospheric Environment*, *42*(33), 7579-7589.

4. The abstract doesn't provide new findings. 1) NPF occurs 50% of all days (if you use a new method to classify NPF events and you compare results with previous methods, it could be a highlight); 2) Events with persistent growth are common in spring and winter; 3) NPF enhances CCN by a factor 1.36, that combined with previous work at SPL, suggests the enhancement of CCN?. These three new findings pointed in the abstract could be results of a measurement report (not for a research paper). The results 1) and 2) have been already reported previously by Hallar et al. 2011.

Response: We are glad that the reviewer brought this point up because by rewriting the abstract, we feel that the main points of the study are more clearly highlighted ensuring that the reader will understand the main findings of this work by just reading the abstract. Additions are reflected on lines 16 – 24.

Addition: ~~Findings show~~ Using the new automatic method to classify NPF, we find that NPF occurs on 50% of all days considered in the study from 2006 to 2021 demonstrating consistency with previous work at SPL. NPF significantly enhances CCN during the winter by a factor of 1.36 and the spring by a factor of 1.54, which, when combined with previous work at SPL, suggests the enhancement of CCN by NPF occurs on a regional scale. We confirm that events with persistent growth are common in the spring and winter, while burst events are more common in the summer and fall. ~~NPF significantly enhances CCN during the winter by a factor of 1.36 and the spring by a factor of 1.54, which, when combined with previous work at SPL, suggests the enhancement of CCN by NPF occurs on a regional scale.~~ A visual validation of the automatic method was performed in the study. For the first time, results clearly demonstrate the significant impact of NPF on CCN in montane North American regions and the potential for widespread impact of NPF on CCN.

Minor Comments

L24-70 – There is a lack of references that have previously investigated the impact of NPF on CCN concentrations, some of them on mountain sites and combining PNSD and CCN and/or using monodisperse (e.g., Kalkavouras et al., 2019; Dameto de España et al., 2017; Kalkavouras et al., 2019; Kalivitis et al. 2015; Kecorius et al. 2019; Rejano et al., 2021; Rose et al. 2017) and some NPF studies in mountain sites.

Response: All the references suggested above are now included in an expanded introduction paragraph (Lines 74-93). The papers listed above that were not included in the first version of the manuscript were re-reviewed to determine additional places throughout the paper where they could be included. We appreciate that the above literature suggestions make the reference list more complete.

Addition: In an effort to increase the number of observational studies relating NPF to CCN, previous studies, both with and without a CCNC, have developed various methodologies to determine the time period in which observed CCN concentrations can be attributed to the occurrence of an NPF event (Kalivitis et al., 2015; Kalkavouras et al., 2017; Dameto de España et al., 2017; Rose et al., 2017; Kalkavouras et al., 2019; Kecorius et al., 2019; Rejano et al., 2021; Ren et al., 2021) Similar to the methodology of Rose et al., (2017), detailed above, Kalkavouras et al., (2017) estimates CCN by finding particle concentrations above the minimum size required for aerosols to activate as CCN and then considers the environmental supersaturation when estimating how many aerosols in a given distribution could act as CCN. This approach further calculates the droplet number and considers how supersaturation, chemical composition, and updraft velocity may impact the cloud droplet number (Kalkavouras et al., 2017). An evolution of this approach by Kalkavouras et al., (2019) calculates the relative dispersion of CCN at different supersaturations and considers CCN times when the relative dispersion is higher than initial conditions before a CCN event (Kalkavouras et al., 2019). This method was further employed at 35 different sites around the globe, both urban and remote, to determine the impact NPF has on CCN concentrations (Ren et al., 2021). Kecorius et al., 2019 utilized a CCNC in the arctic to analyze CCN enhancements by fitting a slope to CCN measurements starting when aerosol formation rates increased and ending when an air mass shift occurred (Kecorius et al., 2019). In another study utilizing a CCNC in Vienna, Austria, Dameto de España et al., (2017) considers CCN number concentrations for a time period that occurs after, and for the same duration as the time difference between NPF initiation and when particles reach CCN relevant sizes (Dameto de España et al., 2017). When it comes to determining the time period that NPF may impact CCN for long term datasets, the methodology should not only efficiently and independently (without using CCN observations) ensure that aerosols are growing to CCN sizes but also needs to consider the growth patterns of individual NPF events to accurately determine when NPF stops contributing to CCN.

L91-99 – CPC model? Do you routinely calibrate the instrumentation? Please, include both information.

Response: Information regarding the specific CPC model and routine instrument upkeep are now included on lines 115-118.

Addition: To measure aerosols at SPL, we use a TSI Inc. (Shoreview, MN) Scanning Mobility Particle Sizer (SMPS) 3936 (with a TSI 3010 Condensation Particle Counter [CPC]) for particles with diameters between 8 and 340 nm that scans every 5 minutes. Data is collected on a log normal scale with particle diameter on a log scale and time on a normal scale. The instrument is periodically shipped back to TSI Inc. for routine maintenance and calibrations.

L104, L107, 108 – These references are mainly based on the methodology presented by Dal Maso et al. (2005).

Response: Additional references to Dal Maso et al., 2005 are now included on lines 135 and 137. Although building off the work of Dal Maso et al., 2005; these references are included because of the progress they make to expand on the number of classification categories which reflects the categories used in this paper.

Addition: In an effort to improve the visual classification process proposed by Dal Maso et al., 2005, studies split events into subcategories to provide more specific classifications detailing whether particle growth is sustained during a given day, or if the given day exhibits a burst of particles (Hirsikko et al., 2007; Kulmala et al., 2012; Boy et al., 2008; Svenningsson et al., 2008; Dal Maso et al., 2005).

Figure 1 – "Is the average concentration below 25 nm above the 10th percentile of all data?" What means? All data serie, 10th percentile of total particle concentration of that 5min data, daily concentrations?

Response: For all days considered by the classification, the average concentration of particles below 25nm is calculated. If a given day's average falls below the 10th percentile of all data, it is assumed that there is not an NPF event due to the lack of particles below 25 nm in the size distribution.

To clarify this step in the process, the box in the flowchart now reads "Is the average concentration below 25 nm of the considered data above the 10th percentile of all data below 25 nm?" This detail is also clarified on Lines 157-159 of the edited manuscript.

Addition: For days ~~with ample~~ where the average particle concentration below 25 nm is above the 10th percentile of all data considered, the maximum of the Gaussians is calculated at each size bin.

L127-136 – The Gaussians are calculated following the equation 1, however, I can not see the diameter parameter. Are you using lognormal distribution? The time index, where is that index? "k" is the maximum aerosol number concentration" for each of the modes I guess?. Please check some references as Huusein et al. 2008 (equations) or Hussein et al. 2005 (DO-FIT algorithm) and rewrite this explanation, difficult to understand which fit method are you applying. In addition, 5 different maximum points? 5 different Gaussians? why that number?

Response: We have made adjustments to the equation and the explanation on lines 159-170 in an effort to make the equation easier to interpret. The new equation reads as follows:

$$f(t \mid k, \mu, \sigma) = ke^{-\frac{(t-\mu)^2}{2\sigma^2}}, \;\; k = max\left(\frac{dN}{dlogD_p}\right)$$

The new format of the equation clarifies that "k" indicates the max number concentration at a given D_p and replaces x with "t" which represents the time at which the normalized maximum number concentration at D_p occurs.

We have further added an explanation to clarify that the non-linear least squares estimate we use is the same one detailed in Bates and Watts 1988. Another aspect that is clarified is the role of D_p (a given diameter midpoint in the size bin). The equation itself does not rely on a D_p value, but rather considers the number concentration over time at a given D_p. It is this distribution that the maximum Gaussian is determined for. We also want to clarify that aerosol data follows a log-normal distribution; with the progression of D_p being on a log scale. Line 117 earlier in the paper now clarifies the scale of the data.

5 different Gaussian maximum points was set as the threshold because the authors deemed anything lower than 5 points an inadequate number of points to run a linear regression. This is important because the linear regression helps calculate growth rate and determine whether the growth of a given day is strong enough to be considered an event. Line 168 now includes a clarification that we consider 5 different Gaussian maximum points.

Additions: The normal distributions were fit by solving for the non-linear least-squares estimates using the R programming language (Equation 1) ~~at~~ which considers the particle size distribution at each diameter to return the time that corresponds to the maximum concentration at that given diameter (Bates and Watts, 1988). In the equation, “k” is the maximum aerosol number concentration, ~~x is a general time index~~ “t” is the time index where the normalized maximum at D_p occurs, “μ” is the mean aerosol concentration, and “σ” is the corresponding standard deviation:

$$f(t \mid k, \mu, \sigma) = ke^{-\frac{(t-\mu)^2}{2\sigma^2}}, \quad k = max\left(\frac{dN}{dlogD_p}\right) \tag{1}$$

The derived time index represents the time at which the maximum of the peak fitted particle size distributions occurs for each ~~respective bin~~ value of D_p. For data where at least 5 different Gaussian maximum points are calculated, a linear regression is fit to these maxima allowing for further analysis of growth over the course of an event (Lehtinen and Kulmala, 2003).

Figure 2 – specify what the black lines indicate (and red ones).

Response: The caption for Figure 2 is rewritten to address what the black and red lines represent.

Addition: An example of a day classified as a class Ib event. Setting 15 nm as the diameter that the growth Gaussian maxima must reach allows for this day to be classified as an event demonstrating why the threshold is set at 15 nm. Gaussian maximums (black points) are outlined by the first-order derivative of the fitted distribution at each size (black line). The vertical red lines denote the initiation and end times of a given event as assigned by the automated methodology

Figure 3 – the authors identify the bottom figure as a weak event, why? There is no new mode appearing below 25 nmor growing.

Response: Thank you for pointing out the error. This was a typo on our part and the bottom plot was always intended to represent a non-event day. The caption for Figure 3 now reflects this change.

Addition: Strong NPF event (top) with midpoint size bin maximums (black points), outlined by the first-order derivative of the fitted distribution at each size (black sloped lines). The vertical red lines denote the initiation and end times of a given event as assigned by the automatic methodology. A ~~weak event~~ non-event (bottom) is added for comparison. The vertical black lines represent the time period when CCN is considered (CCN_{start} through CCN_{end}) which is determined for each individual event day while the seasonal average of this period is used for comparing CCN during non-event days.

Figure 4 – please use log-scale (or log-log)

Response: The authors appreciate the suggestion and we created plots of this relationship on a log scale. After seeing these plots, the authors do believe that the normal scale demonstrates the relationship the best out of all the plots. If we were considering diameters above 100 nm in the specific plot, we would put the x-axis in a log scale. However, because the diameter range we are evaluating is below 100 nm, we believe the normal scale plot is a valid way to demonstrate the data.